Physics of the Geospace Response to Powerful HF Radio Waves

HAARP-Resonance Workshop, 8-9 November 2011

Evgeny Mishin

Space Vehicles Directorate

Air Force Research Laboratory

Integrity ★ Service ★ Excellence

Acknowledgments: Chin Lin, Todd Pedersen of AFRL and Gennady Milikh of UMD

OUTLINE

- ➢ **Introduction**
- ➢ **HF-driven plasma instabilities**
- ✓ **Descending artificial plasma layers:** ***Electron acceleration***
- ✓ **Ionizing wave**
- ✓ **Density ducts and ion outflows:** ***Deficiency of heating***

Cartoon of Artificial Aurora

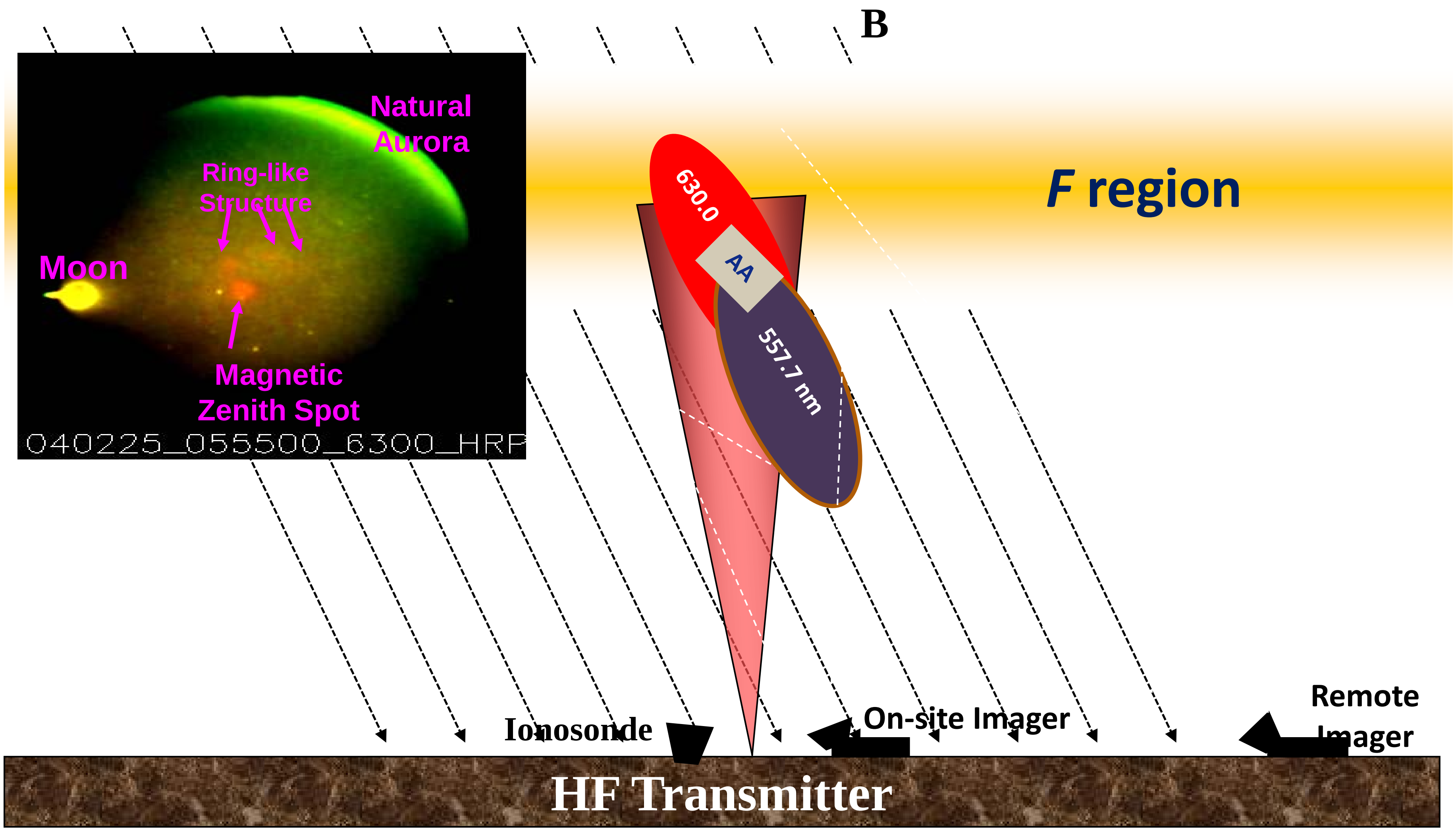

HF Heating

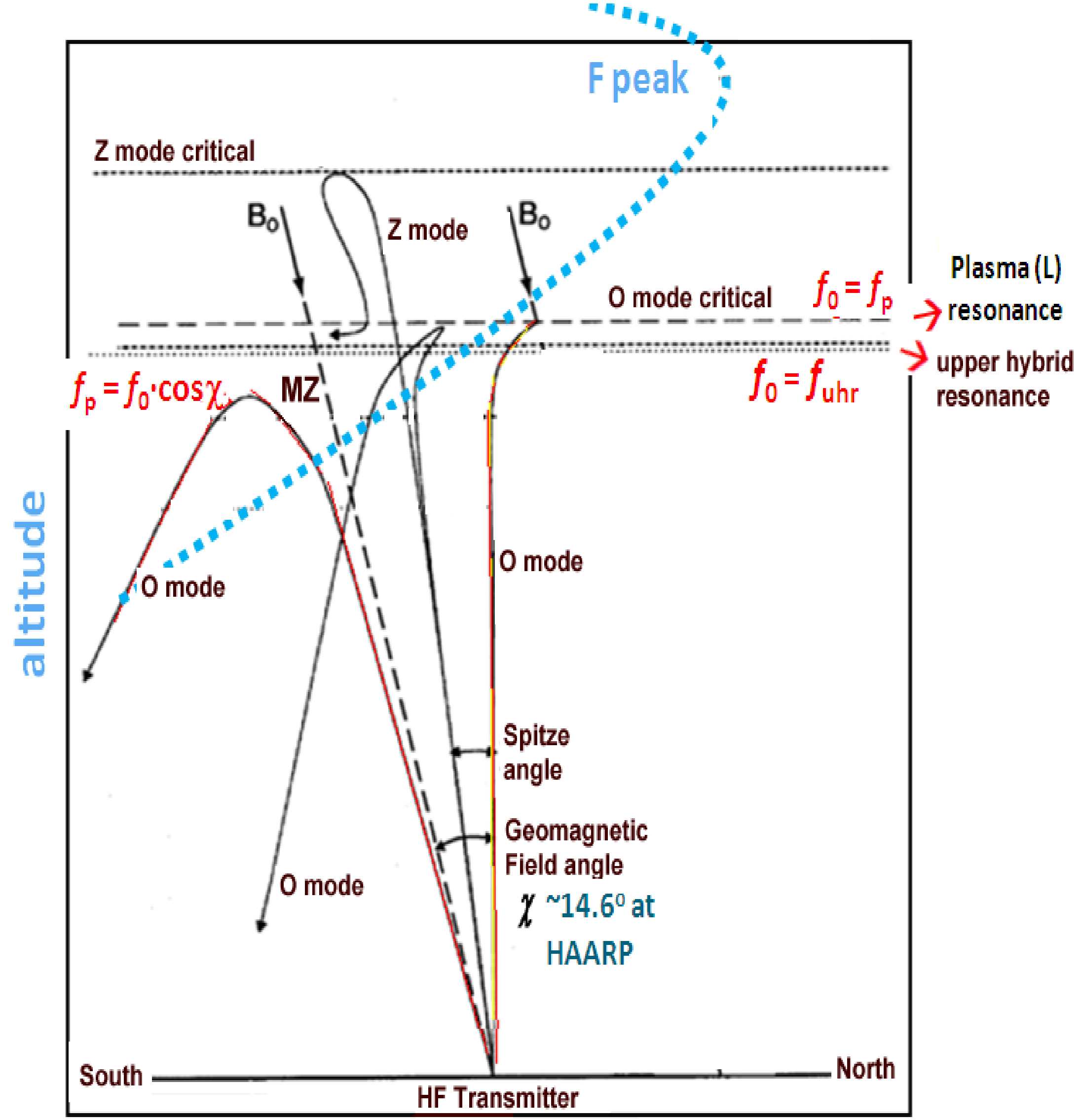

Energy Conversion

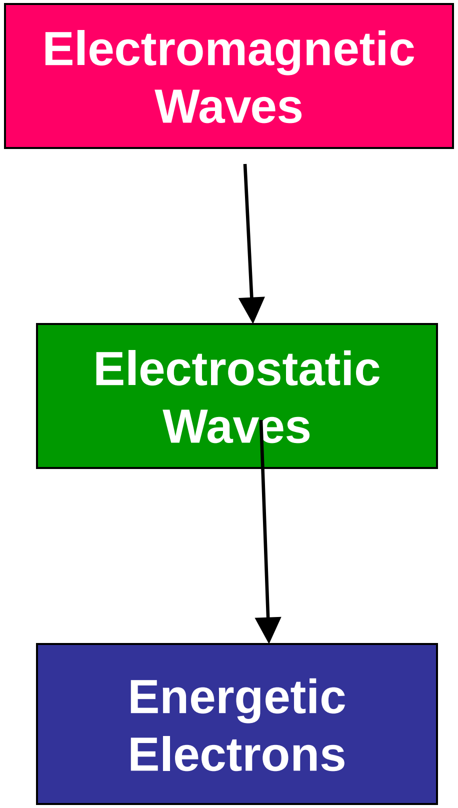

Descending *A*rtificial *P*lasma 'Layer'

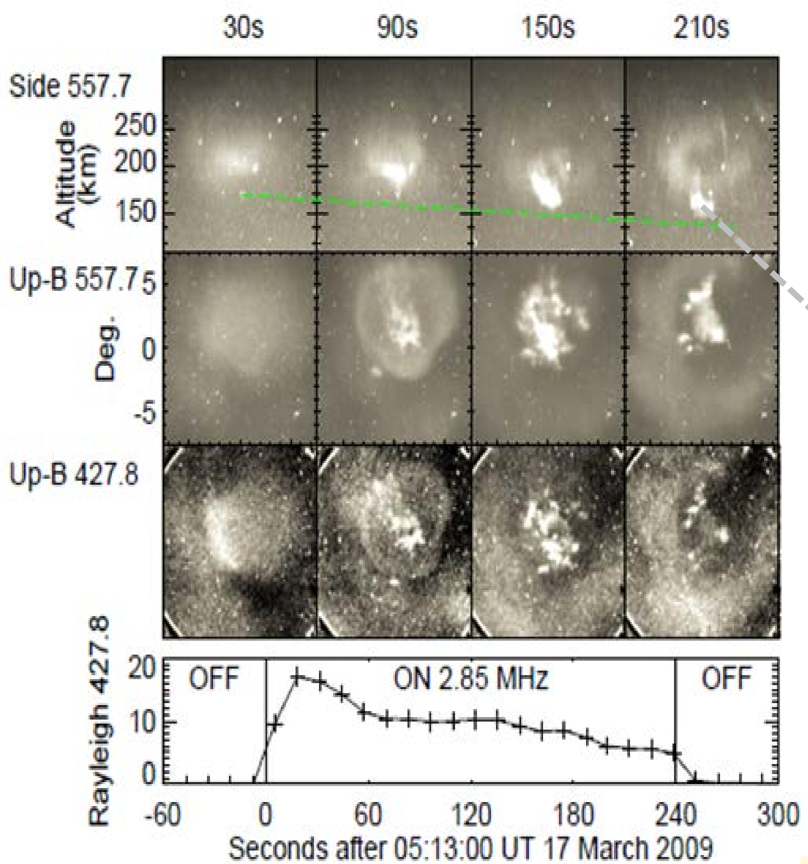

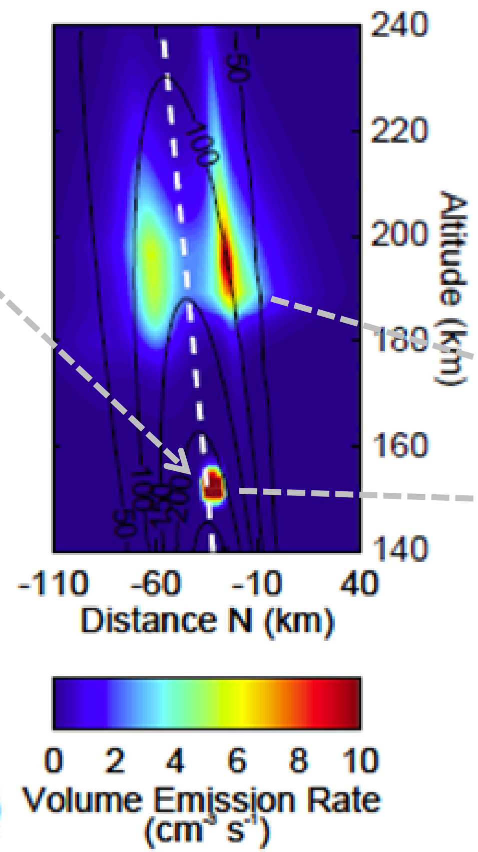

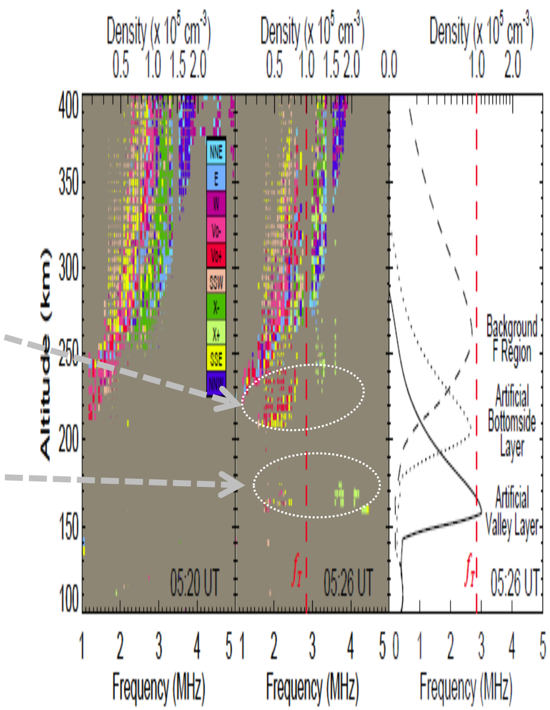

➢1-sec Images of AA from: (top) the remote site at 557.7-nm and the HAARP site looking up along B at 557.7-nm (2nd row) and 427.8 nm (3rd row).

➢4th row: Average intensities at 427.8 nm for the images' center

A tomographic reconstruction of the cross-section of the 557.7-nm volume emission rate for 210 s

▪(left) Ionosonde background echoes (the heater off).

▪(center) Heater on: Two lower layers of echoes near 160 and 200 km virtual height for 210 s.

▪(right) True height profiles.

Pedersen et al., GRL 2010

Optical Ring

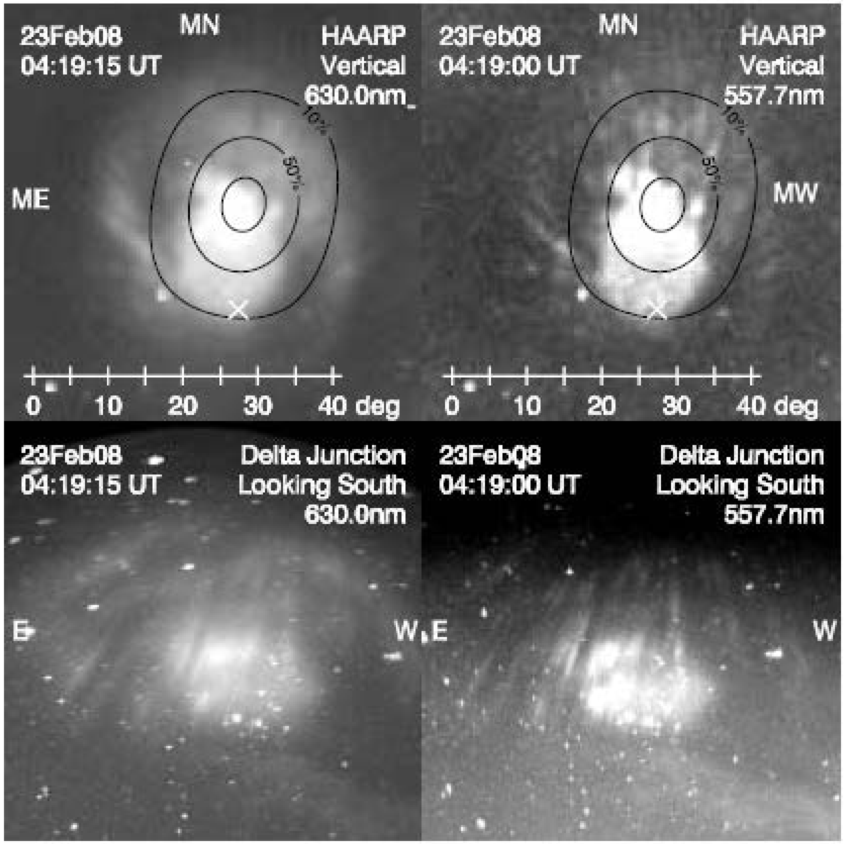

Figure 1. Optical images from the HAARP site looking up (top) and from Delta Junction 160 km N of HAARP looking obliquely S at about 45° elevation (bottom). Contours of the vertical HAARP transmitter beam at 10, 50, and 90% full ERP are superimposed on the data from the HAARP site, along with a scale showing the angular extent of the features.

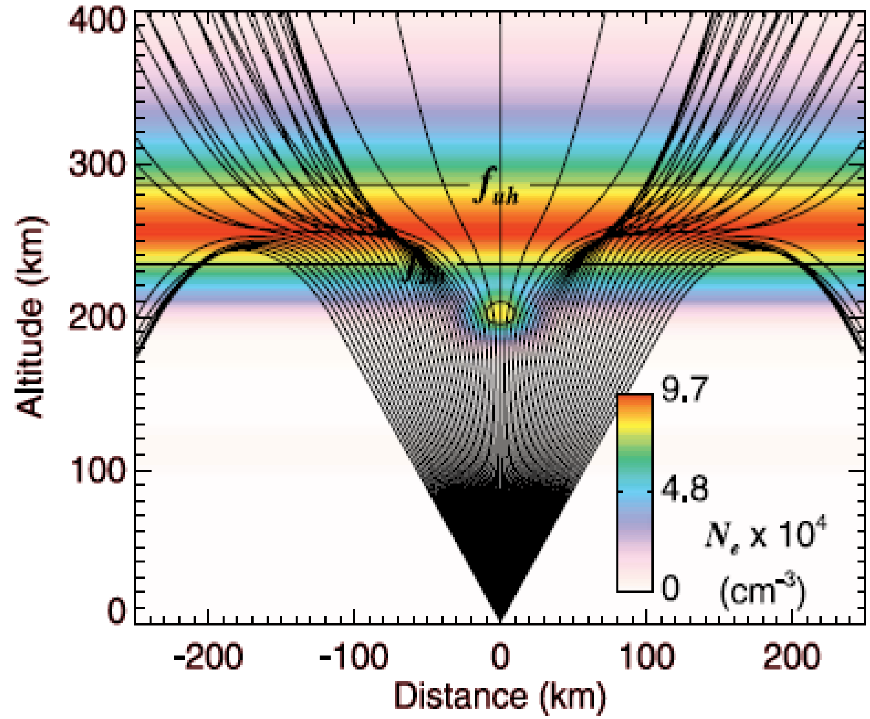

Figure 4. Ray tracing at 2.85 MHz through the background ionosphere perturbed by a localized layer of additional ionization from Figure 2. The concentration of transmitter power to either side of the center would produce a ring when azimuthal symmetry is considered.

Pedersen et al., GRL 2010

Descending Ionizing Wavefront

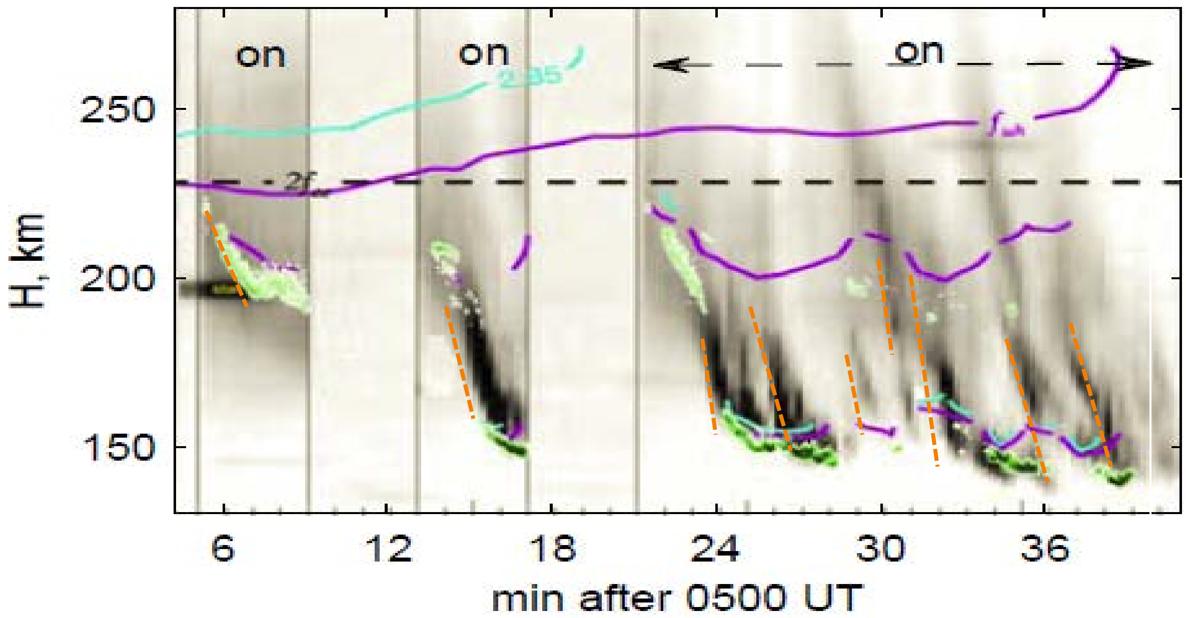

Time-vs-altitude plot of 557.7 nm optical emissions along *B* with contours showing the altitudes where *fp =2.85 MHz (blue)*, *UHR= 2.85* MHz (violet), and $2f_{ce}$ *= 2.85 MHz (dashed white). Horizontal blips* are stars.

Ion Acoustic Line backscatter is shown in green. Red dashed lines indicate Ionizing Wavefronts during heater-on periods (*NB*: Repeatable self-quenching).

Three potential mechanisms :

✓1) suppression of recombination by electron temperature increases

✓2) thermal redistribution of plasma by the electron pressure bulge

✓3) ionization by suprathermal electrons.

➢ *The observed strong optical emissions at 557.7, 777.4, and 427.8 nm are most consistent with (3)*

Mishin & Pedersen , GRL 2011

Accelerated Electrons & Ionization

▪Near 180 km the plasma frequency in the descending layer reaches f_0 or $n_e=n_c$ blocking propagation of the HF beam above the artificial layer. The artificial plasma is now completely self-sustained and rapidly propagates along the magnetic field downward as the ionizing wave front due to ionization by accelerated electrons.

$$F_a^{\|}(\varepsilon_{\|}) \simeq n_a(2p_a-1)/v_{\min}\cdot(\varepsilon_{\min}/\varepsilon_{\|})^{p_a}$$

$$\langle \nu_{ion}\rangle \approx \kappa_{ion}^{*}\cdot\left([N_2]+\tfrac{1}{2}[O]+0.95[O_2]\right)\ \mathrm{s}^{-1}$$

$$\kappa_{ion}^{*} = \langle v\sigma_{ion}\rangle/n_a \approx 1.8\cdot 10^{-8}\ \mathrm{cm^3 s^{-1}}$$

$$\varepsilon(\varepsilon_0,\xi) \simeq \varepsilon_0 - \int_{h_0}^{h_0+\xi} L(\varepsilon(z))\sqrt{2/\delta_e(\varepsilon(z))}\,dz$$

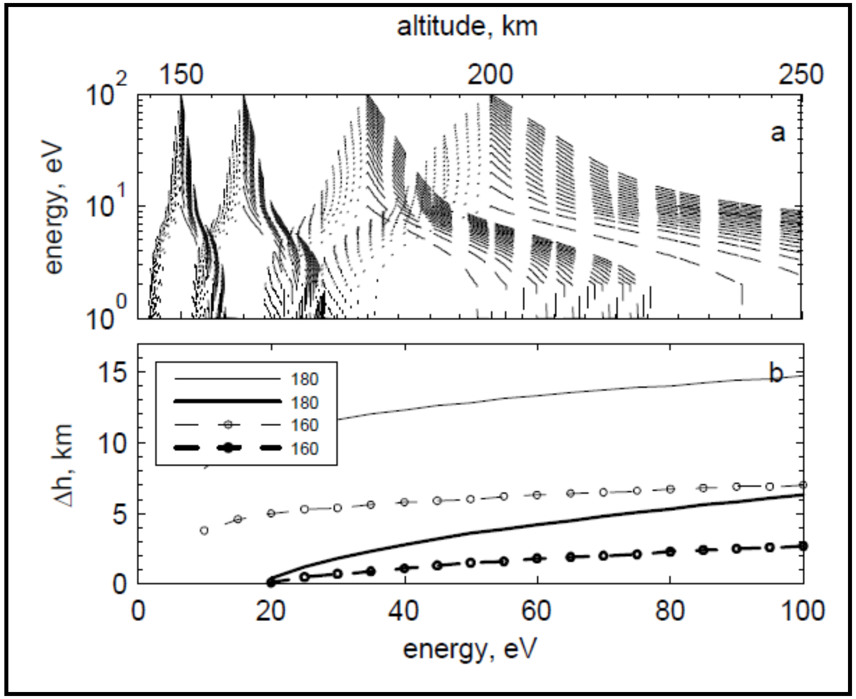

(a) Altitude profiles $\varepsilon(\varepsilon_0,h)$ at ε_0 =10, 15, ...100 eV and h_0 =150, ...200 km.
(b) Half-widths Δ_g (thin lines) and Δ_b (thick) of the green- and blue-line excitation layers near h_c =160 (circles) and 180 (solid lines) km.

Mishin & Pedersen, GRL 2011

Ionizing Wave

At each time step artificial ionization occurs near the altitude h_c, where n_e=n_c. The density profile just below h_c is represented as

$$n_e(x,t_i) = n_c \cdot \Psi(x)$$

$\Psi(0) \geq 1$ and $\Psi(x) \ll 1$ at $x > 1$

$$x = \xi / L_{\|},\ \xi = (h_c - h)/\cos\alpha_0$$

Distance along ***B***

$$L_{\|} \simeq \left\langle l_{ion}\sqrt{\delta_e/2}\right\rangle$$

Average ionization length

Ionization by accelerated (subscript *a*) electrons increases the plasma density near ***h_c***

$$n_e(x_i, t_i + \Delta t) \simeq q_a(\xi_i)\cdot\Delta t \qquad q_a = n_a \cdot \langle \nu_{ion}(\varepsilon)\rangle$$

$$T_{ion}^{-1} \simeq q_a/n_c$$

Ionization time

Speed of descent

$$V_d = |dh_c/dt| \simeq L_{\|}T_{ion}^{-1} \simeq \left\langle v\sqrt{\delta_e/2}\right\rangle n_a/n_c$$

$$\left\langle \delta_e^{1/2} v\right\rangle \simeq 1.5\cdot 10^6 \text{ m/s} \longrightarrow n_a \simeq 6\cdot 10^{-4} n_c$$

In excellent agreement with the optical observations

Ducts and Ion Outflows

Density ducts

O^+/n_e ratio

Ion vertical velocity

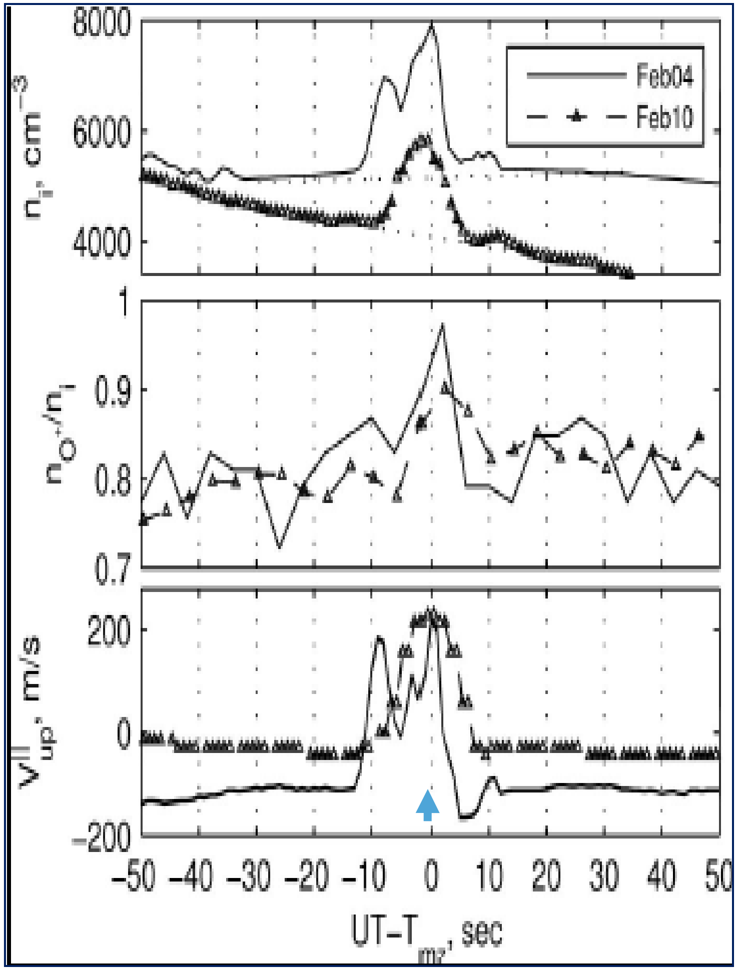

Milikh et al., GRL, 2010

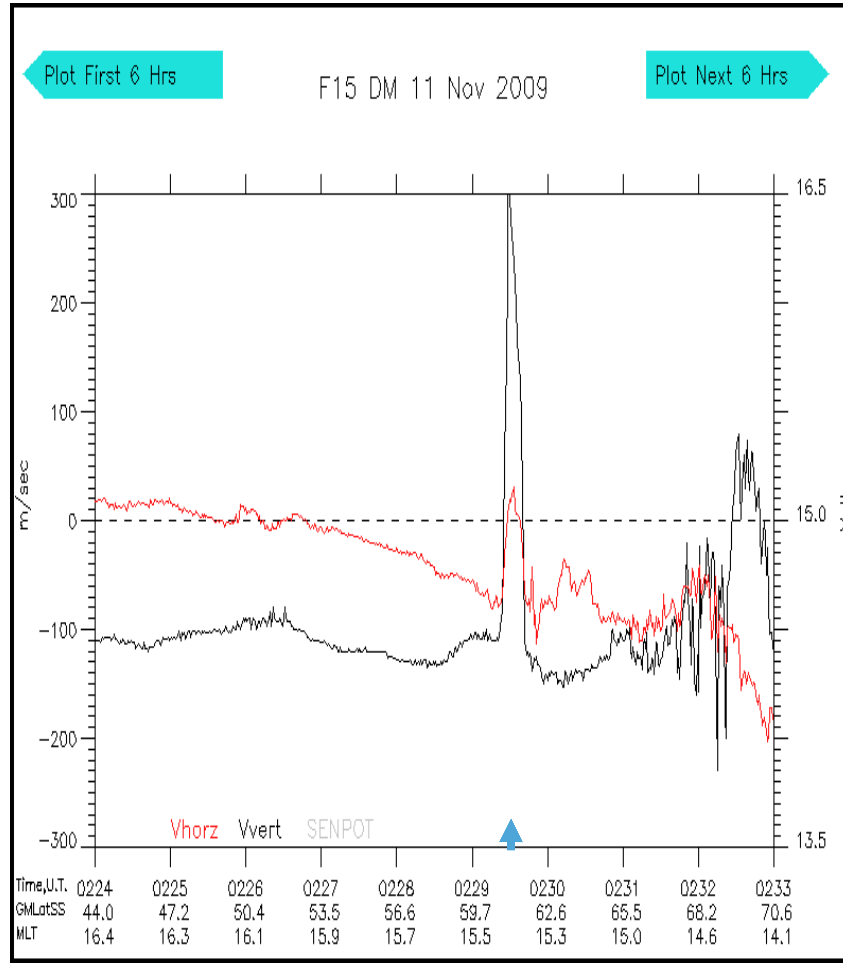

Observed during the period of descending APLs

Simulations

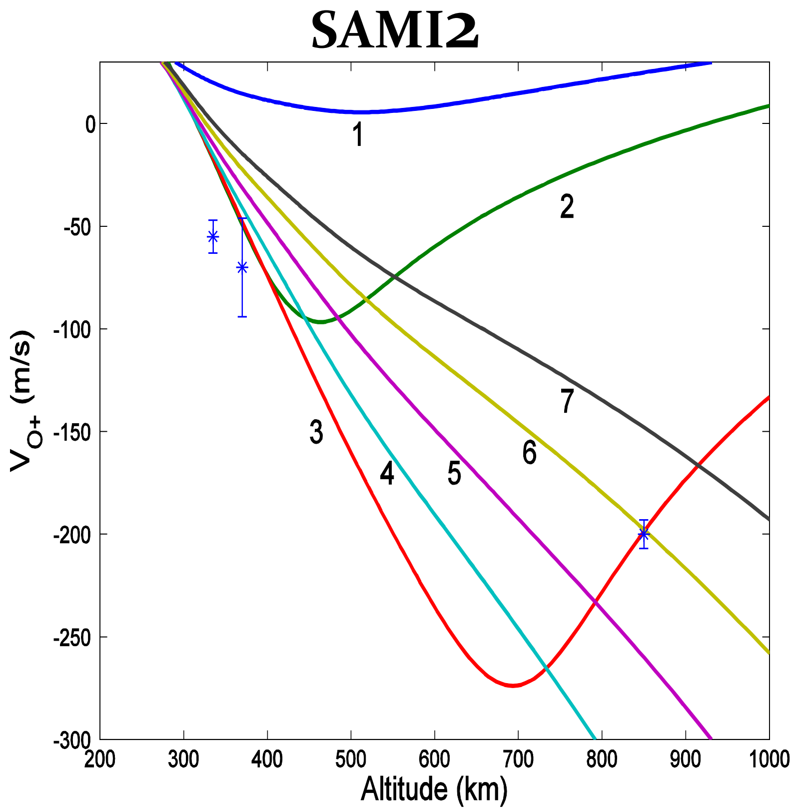

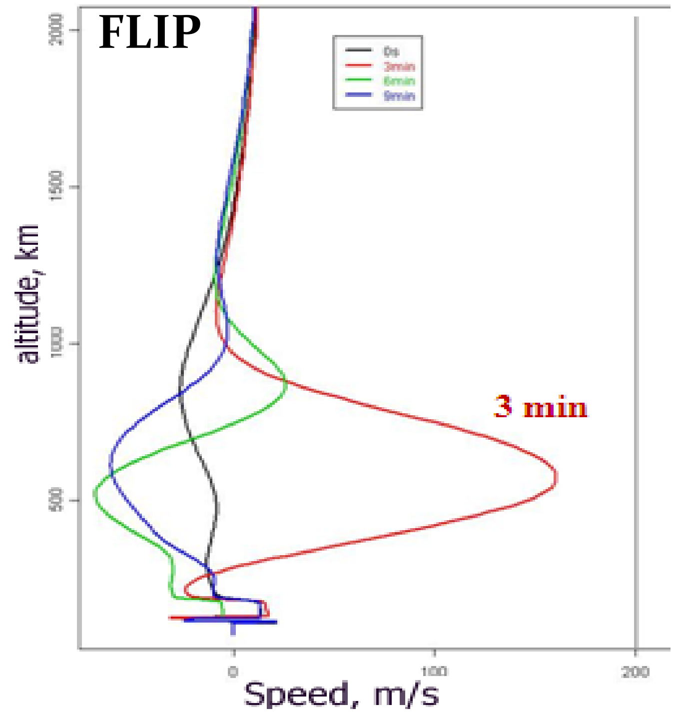

- 2-min steps.
- Two experimental values on the left are from ionosonde skymaps and that on the right is from DMSP F15.
- Match after 6 min in the strongest heating.

Before heating (t = 0) ions drift downward at < 20 m/s.

During heating (t= 3 min) ions drift upward at altitudes from 300 km to 1000 km and reach 160 m/s at 600 km.

After heating (t = 6 min) ions drift downward below 800 km and upward at higher altitudes

After cooling (t = 9 min) ions move downward

Milikh et al., GRL, 2010

Simulation vs. observations

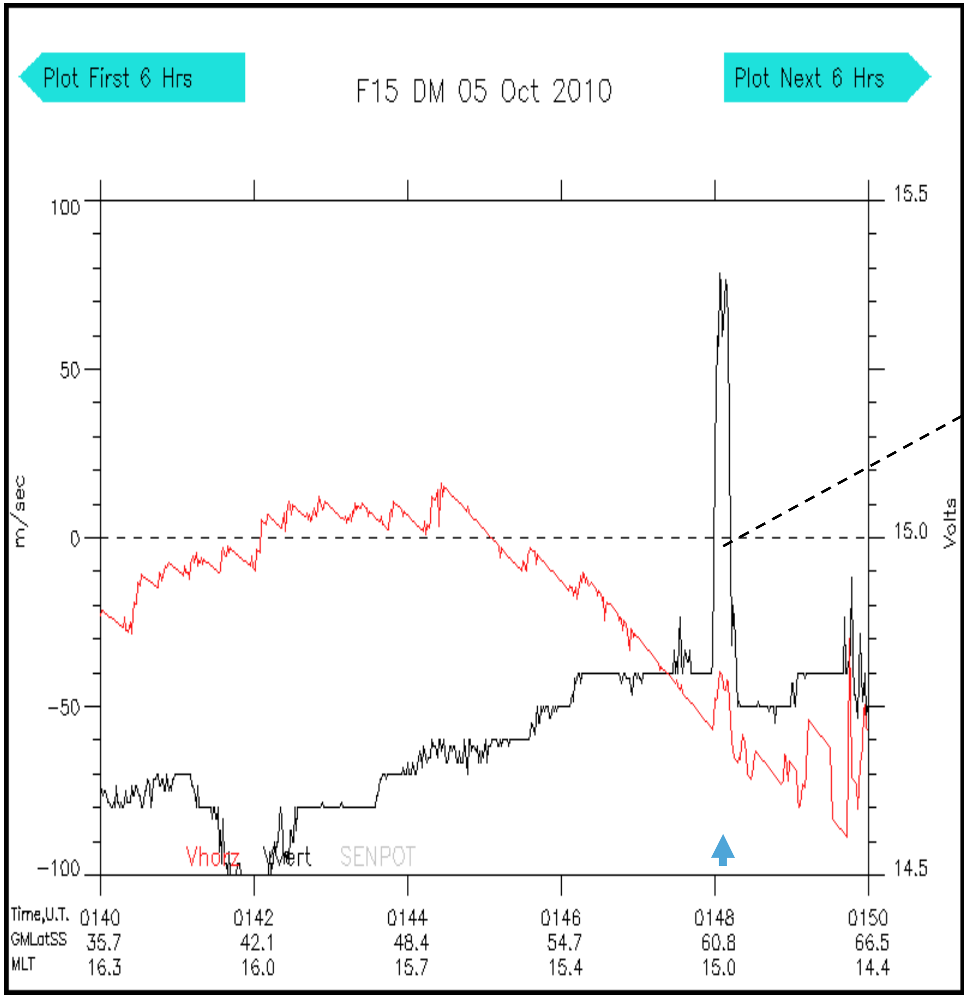

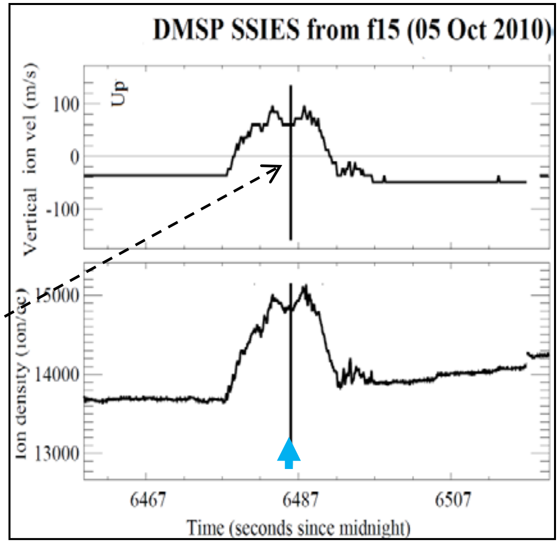

- ➢Contradicts to the conventional *fluid* models
- ➢Requires that heat transfer or/and suprathermal effects be accounted for.

Observed in *only* 3 min in the heating
→ 3 km/s upward propagation speed

Summary

- The HF-driven ionization process is initiated near 220 km altitude in the ambient F layer. Once the artificial plasma reaches sufficient density to support interaction with the transmitter beam it rapidly descends as an ionization wave to ~150 km altitude. Ionizing wave model due to HF-accelerated electrons explains the observations.

➢ 2-3 km/s speeds needed to explain the fast appearance of artificial ducts and ion outflows in the topside ionosphere contradict to the conventional (fluid) models.

➢ Point to suprathermal populations and/or heat transfer processes.

EISCAT UHF radar observations